HHS Public Access

Author manuscript

Cryo Letters. Author manuscript; available in PMC 2023 May 16.

Published in final edited form as:

Cryo Letters. 2020 ; 41(4): 185–193.

CRITICAL COOLING AND WARMING RATES AS A FUNCTION OF CPA CONCENTRATION

Zonghu Han[1], **John C. Bischof**[1,2]

[1]Department of Mechanical Engineering, University of Minnesota, Minneapolis, USA

[2]Department of Biomedical Engineering, University of Minnesota, Minneapolis, USA

Abstract

Cryoprotective agents (CPAs) are routinely applied in cryopreservation protocols to achieve the vitrified state thereby avoiding the damaging effects of ice crystals. Once the CPA has been added, the system needs to cool at a rate ≥ critical cooling rate (CCR) to avoid ice crystallization and successfully enter the vitrified state. Subsequently, upon warming the system needs to meet or exceed a critical warming rate (CWR), often one to two orders of magnitude higher than the CCR, to avoid ice formation and return the system to physiological temperatures for use. Many experimental and theoretical studies have been published on CCRs and CWRs, and correlation for these rates as a function of concentration has been explored for some single component CPAs, but not the CPA cocktails which are commonly used in tissue and organ cryopreservation. In this paper, we summarize the available data of CCRs and CWRs for a variety of CPAs, and suggest a convenient mathematical expression for CCR and CWR that can guide general use for cryoprotective protocol, but also highlights the critical need for further study on CPA cocktails and tissue systems in which CPAs may behave differently and/or may not be fully equilibrated to the loaded CPA.

Keywords

tissue and organ vitrification; plant vitrification; critical cooling rates; critical warming rates; cryoprotective agents

INTRODUCTION

Vitrification, as a means of cryopreservation, has been used with rapidly expanding frequency due to its distinct advantage – it can completely eliminate the ice formation and its consequent damage. Since 1984 when a practical universal approach to vitrification was proposed by Fahy (26), a variety of biological systems has been vitrified, e.g., embryos (62), veins (70) and arteries (4), and kidneys (26). The success of vitrification relies on successfully entering and returning from the vitrified state which requires the sample to exceed the critical cooling rate (CCR) and critical warming rate (CWR), which are the minimum rates to suppress ice formation during the cooling and rewarming process, respectively. CCRs and CWRs mainly depend on the CPA formulation and concentration. In general, for a given CPA, lower concentrations require high cooling rates and even higher warming rates to avoid ice formation. For instance, for tissue and organ cryopreservation,

the three most commonly used CPA cocktails (DP6 (6 M), VS55 (8.4 M), and M22 (9.3 M)) have CCRs of 40 °C/min (23), 2.5 °C/min (49), and 0.1 °C/min (29), and CWRs of 189 °C/min (85), 50 °C/min (70), and 0.4 °C/min (28), respectively. However, we lack data for diluted CPA cocktails, which is the most frequent situation in tissue and organ cryopreservation since tissues normally aren't equilibrated to the base CPA concentration. For instance, Manuchehrabadi and Gao et al. have shown that even after 180 min loading with VS55, the 0.8 mm carotid artery was still not equilibrated (45), while the practical loading protocol is normally much less than that time due to the toxicity effect of CPA exposure (46).

Previous work has studied the relationship between CCRs and CWRs vs concentration of single component CPAs (27, 53, 79), with a summary of this data re-plotted in Figure 1a and b. Concentrations are given in % w/w (CPA weight by solution weight). The conversion from C (concentration in % w/w) to M (molarity) is, $M = C/W/(C/\rho_{cpa}+(1-C)/\rho_{water})$, where W is the molar mass of the CPA, ρ_{cpa} and ρ_{water} are the densities of CPA and water respectively. For example, for DMSO, the concentrations of 20, 40, 60, and 80% in w/w correspond to 2.61, 5.31, 8.12, and 11.05 mol/L respectively. The data (and extrapolations) show that lower CPA concentrations require higher CCRs, and even higher CWRs (12, 36, 78). While valuable, this data is focused on only a few CPAs, mostly at CPA concentrations larger than 30% due to the cooling and heating ability of existing DSCs (74). Recently, researchers have developed new cooling and heating methods and measured the CCRs and CWRs in the lower CPA concentration region (lowest at 18%) (11). This brief communication reviews all available data at all rates available for single component CPAs, to establish a general relationship between their CCRs and CWRs, which can provide a reference for the diluted CPA cocktails and other CPAs that are lacking direct measurement data.

CCR, CWR measuring method

To determine CCR and CWR, researchers have to cool down and warm up the sample, respectively, record the thermal history and then detect ice formation during the cooling or warming process. Cooling and warming can be achieved by differential scanning calorimetry (DSC), plunge cooling/warming, fast scanning calorimetry and laser calorimetry, as listed in Table 1.

Ice formation can be detected by visual inspection (11, 34, 81), X-ray diffraction measurements (11, 21, 32, 48, 81), and calorimetry measurements (13, 75). Calorimetry measurements can quantify the ice formation dynamically and precisely, but traditional DSC cannot achieve cooling or warming rates more than 160 °C/min (6, 74, 81). Visual inspection, which can be combined with X-ray diffraction at liquid nitrogen temperatures, can detect ice formation during rapid plunge-cooling and warming [i.e., high speed video microscopy (38, 73)]. However, visual inspection cannot quantify the amount of ice formation, only whether or not it occurred and XRD is usually just used at the cooling end point to assess the presence of crystalline vs. amorphous phase [i.e., not a dynamic measurement (11, 21, 35, 48)].

DSC can be used to determine both the CCR and CWR. For CCR determination, researchers apply different cooling rates, v_{cr} (°C/min), ranging from 2.5 to 160 °C/min to cool down the sample, and record the heat of ice crystallization, q, for each cooling rate. They plot q vs v_{cr} and fit into the model developed by Boutron (12) to obtain the two constants in the model, q_{max} (maximum heat of ice crystallization) and k_4 ($\propto$ CCR), which represents the glass-forming tendency of the specific CPA at the specific concentration (7, 9, 18, 60). Then one can theoretically calculate the quantity of ice formation at any rate. The CCR by this method is defined as the point on the theoretical curve corresponding to 0.2% ice formation in the solution (13).

CWR defined by the DSC method is the warming rate required to confine crystallization to approximately 0.2~0.5% of the mass of an average sample (13, 29). For practical purposes, the CWR can be defined as the rate at which $T_m/T_d = 1.05$, where T_m is the melting temperature and T_d is the devitrification peak, which is an increasing function of warming rate (60). T_m/T_d varies linearly with warming rate in log scale, log(v_{wr}), in agreement with theory within a good approximation between 2.5 and 80°C/min (17, 43, 44). Warming rates larger than 160 °C/min are too high to be observed in DSC, therefore they have typically been estimated by extrapolation (17).

For plunge cooling and warming (11, 34, 81), researchers used different sizes of sample holders (e.g. CryoLoops, capillaries of different diameters) to create different sizes of CPA samples in order to obtain different cooling and warming rates. Cooling and warming are done by rapidly inserting the samples into liquid nitrogen and hot oil, respectively. The thermal history, recorded by thermocouples, is applied to estimate the cooling and warming rates. Ice formation is assayed by judging sample transparency/opacity, i.e., visual inspection. X-ray diffraction is often used as a supplement to visual inspection after plunge cooling, to confirm the transparent/opaque transition corresponds to the glass/crystal transition.

Future work may be able to take advantage of faster calorimetry techniques based on nano and laser calorimetry. For instance, nanocalorimetry is a thin film sensor technique that can reach 10^5 – 10^6 °C/min (1, 22, 86, 87). A small mass of sample (nano-grams) is placed on a flat thin membrane with a film-heater. A film-thermopile sensor is placed next to the heater to record the temperature history. The sample is cooled by the ambient helium or nitrogen gas, which serves as cooling agent providing the heat transfer between the sample and the thermostat (50, 51, 52, 88). This technique, or modifications of it, can achieve very fast cooling and warming rates, and may well be useful in assessing CCRs and CWRs of CPAs and CPA loaded tissues warmed by metal forms which can approach 1000s °C/min (46). Another calorimetry approach can use laser absorption to estimate CWR in aqueous droplets (38). Here the cooling process leverages existing approaches (i.e. plunge liquid nitrogen cooling), however, warming is governed by laser absorption within a droplet which has well characterized plasmonically active nanoparticles that heat with known efficiency [$SAR = C_{abs} \cdot N \cdot I = \mathrm{W/m^3}$, where C_{abs} is the absorption cross section ($\mathrm{m^2}$), N is the number of GNP/$\mathrm{m^3}$, I is laser fluence rate ($\mathrm{W/m^2}$)] (61). By changing the GNP concentration and the laser irradiation, a broad range of warming rates can be reached (10^3~10^7 °C/s).

Ice formation during cooling can be observed visually or by XRD. Ice formation during warming can be recording by high-speed video.

CCR, CWR vs concentration correlation

Figure 1c and d summarized the CCR and CWR to avoid ice formation during cooling and rewarming in various CPAs obtained from all available sources. From Fig. 1c, one can see the same trend for all kinds of CPAs as in Fig. 1a: the lower the CPA concentration, the higher the cooling rate required for vitrification.

The two parameters, q_{max} and k_4, obtained from Boutron's CCR model represents the glass-forming tendency in a specific CPA based on concentration, i.e., larger concentration CPA has better glass-forming tendency and smaller q_{max} and k_4. However, as cocktails are increasingly being used such as DP6, VS55 and M22, there is a need for a general prediction based on concentration alone. Furthermore, as tissues are increasingly perfused or diffused with CPA cocktails for vitrification, the actual concentrations reached within the tissue will be only a fraction of the loading concentration of the cocktail, thereby further necessitating a simple relationship for rates vs. concentration (3, 45, 46). To achieve this we plotted all the available data points for all single component CPAs (intentionally ignoring variations between CPAs) and found a simple relationship (shown in Fig. 1c), $\left(R^2 = 0.64\right)$,

$$v_{ccr} = 1 \times 10^7 \cdot e^{-0.269 \cdot C} \quad [1]$$

where C represents CPA concentration (w/w) and v_{ccr} stands for the critical cooling rate (°C/min).

Since an intrinsic relationship between CCR and CWR is expected, we plotted the CWRs and CCRs of CPA aqueous solutions together in Figure 1d and found a roughly linear regression between them $\left(R^2 = 0.69\right)$, shown as the solid line in Fig. 1d.

$$v_{cwr} = 3.775 \cdot {v_{ccr}}^{2.377} \quad [2]$$

where v_{cwr} is the critical warming rate (°C/min).

While CCR and CWR data has been generated for many single component CPAs (Fig. 1) there is much less data available for CPA cocktails. To illustrate this, we have taken CCR and CWR data points from three commonly used CPA cocktails (DP6, VS55 and M22) and plotted them in Fig. 2. We then superimposed the single CPA fit extrapolations from Fig. 1. One notices that the CCR prediction fits reasonably well $\left(R^2 = 0.94\right)$, while the CWR fit is much less descriptive $\left(R^2 = 0.38\right)$. This may be due to the use of saccharides in the cocktails which are prepared in sugar-rich carrier solutions: DP6 and VS55 in Euro-Collins (EC) (19, 77), and M22 in LM5 (29). The sugar component is expected to have a significant effect on CWR, but much less on the CCR (discussed in the following section), so this could explain the observed difference in behavior. However, in the absence of more data from specific cocktails these first order estimates can be used to extrapolate to lower concentrations to

predict CCRs or CWRs for diluted cocktails (i.e., potentially helpful in partially equilibrated tissues and other systems).

Modification of CCR and CWR (CPA type, Carrier Solution, Tissue).

Although Eqns. [1] and [2] establish a simple relationship for protocol development, further refinement of these equations to account for CPA type, carrier solution and tissue loading are needed. For instance, sugars (e.g. glucose, trehalose and sucrose) and other polymers that are routinely included in vitrification solutions (31, 33, 40, 42, 71) can increase the glass transition temperature (41, 69), the glass-forming tendency and the stability of the amorphous state (9, 30), all of which will reduce the CCR and CWR (76). Carrier solutions containing salts and sugars as osmotic buffers (63) have the same effects; sugar-rich carriers [e.g., Euro-Collins and LM5 (29, 49)] can also drastically decrease CCR and CWR of CPAs, whereas salt-rich carriers (e.g., PBS and St Thomas solution) have a smaller effect (9, 53). For instance, Euro-Collins decreased the CCR for 30% 2,3-BD from 272 to 49 °C/min (over 5-fold), and CWR from 1×10^8 to 4×10^4 °C/min (2500-fold), while PBS only decreased the CCR to 162 °C/min (1.6-fold) and the CWR to 1.1×10^7 °C/min (9-fold) (9). Further study on the mechanisms of action for these individual components is likely needed to identify a better fit to the complete behavior of CPA cocktails.

Tissue permeated with CPAs can further increase the glass-forming tendency and the stability of the amorphous state compared to CPA diluted with carrier solution, leading to a decrease in the CCR and CWR (60). In Peyridieu et al (60), kidney tissues permeated with EC diluted 30% 2,3-BD decreased the CCR from 49 to 3 °C/min (~16-fold) and the CWR from 4×10^4 to 100 °C/min (400-fold). This behavior might be due to the compartmentalization of the solution in the tissues, which is very similar to that of the compartmentalized water in hydrogels with pore sizes on the order of nanometers (54, 55), leading to a confining effect that can decrease the crystallization tendency of water (59). This might also be similar to an isochoric process (64), where the tissue surface forms a vitrified shell that builds up the internal pressure while cooling (82). While the general trends are expected to continue from basic study of the CPA cocktails, this suggests that specific study of CPA performance in tissue systems is also needed.

Plant vitrification

Hardy plants are uniquely well adapted to resist extreme cold in the nature (83). For hardy plants cryopreservation, samples are preforzen at a temperature varying from −15 to −40 °C (depends on the relative hardiness of the plant) for hours to freeze dehydrate the hardy cells, and then immersed in LN_2. However, for less or nonhardy plants cryopreservation, vitrification technique was applied (24, 66). Samples are first loaded with intermediate concentration CPA (usually 2 M glycerol + 0.4 M sucrose) (57, 68), and then loaded with the high concentration plant vitrification solution (PVS) for dehydration. Then the samples are cooled by direct immersion in LN_2 (cooling rate: about 200 °C/min) and then rapidly warmed by water bath (warming rate: about 250 °C/min) (65). The derived encapsulation-vitrification (47) and droplet-vitrification (37) were developed for easier manipulation and faster rates.

Plant vitrification solutions designed by Sakai et al. were most commonly used, especially PVS2 and PVS3. PVS1 [22%(w/v) glycerol, 15%(w/v) ethylene glycol, 15%(w/v) propylene glycol and 7%(w/v) DMSO, and 0.5M sorbitol] was designed for asparagus cultured cells and somatic embryos (80), PVS2 [30%(w/v) glycerol, 15%(w/v) ethylene glycol and 15% (w/v) DMSO and 0.4 M sucrose] was designed for citrus callus (67), and PVS3 [50% (w/v) glycerol and 50% (w/v) sucrose in water] was designed for asparagus embryogenic suspension cells (58). Those PVS cocktails and some modified versions (39) has been applied to the vitrification of a wide range of plant materials of both temperate and tropical origins, more than 200 plant species (66).

The exposure of samples to PVS was simply considered as a dehydration process due to the short duration (mostly < 1 hour), where CPAs were assumed not able to penetrate the cytosol of the explant cells and they only have an osmotic action (25, 67, 72). Therefore, the key to the success of vitrification was to carefully control the dehydration procedures and to prevent injury by chemical toxicity or excessive osmotic stress during treatment with the PVS solution (66), and lots of work focused on optimizing the time and temperature of exposure to PVS. However, not too much work focused on the PVS thermal properties and permeation. The simplification of a pure dehydration might not be accurate for a fairly long loading time, and some groups developed a rapid way of PVS permeation (56), which means there must be CPA in the cell cytosol and makes the cell behave like the applied CPA. Therefore, the properties of PVS need to be studied. There are reported glass transition, devitrification and melting temperatures for PVS2 (67), but CCRs and CWRs were not measured for any of the PVS. Based on this review (Fig 1 c and d), PVS1 [61.75% (w/w) CPA], PVS2 [64.54% (w/w) CPA], and PVS3 [77.5% (w/w) CPA] have CCRs of 0.611, 0.288, and 0.01°C/min, and CWRs of 1.17, 0.196, and 6×10^{-5} °C/min, respectively. Benson et al. confirmed that CCR for PVS2 is less than 10 °C/min by DSC (10), which is in agreement with our estimation. However, based on the fact that exposure is used primarily for dehydration and may not lead to full equilibration (i.e., not fully permeated) these rates may be lower than actually needed.

The CCR and CWR curves shown in this study may provide a good reference for optimizing the PVS concentration and loading time for plant tissues therefore decreasing the toxicity and osmotic shock, and guiding the cooling and warming protocols to achieve the estimated rates.

CONCLUSION

In conclusion, this work reviews the available data for the CCRs and CWRs for CPAs. For simplicity and protocol development we were able to plot and represent the available data with a simple relationship for available single component CPAs that relates CCR and CWR to concentration. While the fit is relatively rough and incomplete, it can still provide a first-order guide to predicting behavior in CPA cocktails and tissue systems. This review identifies several important opportunities for further work in this area including: 1) the need for data at low concentrations [< 20% CPA w/w)], 2) a need to include the effects of saccharides and tissue loading on the reduction of CCRs and CWRs, and 3) the eventual need to develop relationships for specific CPA systems. All of these issues suggest the

need for additional experimental (and theoretical) work on CCR and CWR in the future for specific CPAs, CPA cocktails and partially or fully CPA equilibrated tissues.

REFERENCES

1. Adamovsky S, Minakov A & Schick C (2003) Thermochimica Acta 403, 55–63.
2. Arnaud FG, Khirabadi B & Fahy GM (2003) Cryobiology 46, 289–294. [PubMed: 12818220]
3. Baicu S, Taylor M, Chen Z & Rabin Y (2006) Cell Preservation Technology 4, 236–244. [PubMed: 18185850]
4. Baicu S, Taylor M, Chen Z & Rabin Y (2008) Cryobiology 57, 1–8. [PubMed: 18490009]
5. Bald W (1986) Journal of Microscopy 143, 89–102. [PubMed: 3531522]
6. Baudot A, Alger L & Boutron P (2000) Cryobiology 40, 151–158. [PubMed: 10788314]
7. Baudot A & Boutron P (1998) Cryobiology 37, 187–199. [PubMed: 9787064]
8. Baudot A, & Odagescu V (2004) Cryobiology 48, 283–294. [PubMed: 15157777]
9. Baudot A, Peyridieu J, Boutron P, Mazuer J & Odin J (1996) Cryobiology 33, 363–375. [PubMed: 8812102]
10. Benson E, Reed B, Brennan R, Clacher K & Ross D (1996) CryoLetters 17, 347–362.
11. Berejnov V, Husseini NS, Alsaied OA & Thorne RE (2006) Journal of Applied Crystallography 39, 244–251.
12. Boutron P (1986) Cryobiology 23, 88–102. [PubMed: 3956232]
13. Boutron P (1993) Cryobiology 30, 86–97.
14. Boutron P & Kaufmann A (1979) Cryobiology 16, 83–89. [PubMed: 436443]
15. Boutron P & Kaufmann A (1979) Cryobiology 16, 557–568. [PubMed: 544180]
16. Boutron P, Kaufmann A & Van Dang N (1979) Cryobiology 16, 372–389. [PubMed: 487853]
17. Boutron P & Mehl P (1990) Cryobiology 27, 359–377. [PubMed: 2203605]
18. Boutron P, Mehl P, Kaufmann A & Angibaud P (1986) Binary systems water-polyalcohol. Cryobiology 23, 453–469. [PubMed: 3769520]
19. Brockbank KG, Chen Z, Greene ED & Campbell LH (2015) in Cryopreservation and Freeze-drying Protocols, Methods in Molecular Biology (Methods and Protocols), vol 1257, (eds) Wolkers W & Oldenhof H, Springer, New York, pp. 399–421.
20. Brüggeller P & Mayer E (1980) Nature 288, 569.
21. Chinte U, Shah B, DeWitt K, Kirschbaum K, Pinkerton A & Schall C (2005) Journal of applied crystallography 38, 412–419.
22. De Santis F, Adamovsky S, Titomanlio G & Schick C (2006) Macromolecules 39, 2562–2567.
23. Eisenberg DP & Rabin Y (2015) Journal of Biomechanical Engineering 137, 081007. [PubMed: 25839134]
24. Engelmann F (1997) Plant Genetics Resources Newsletter 112, 9–18.
25. Engelmann F & Takagi H (2000) in Cryopreservation of Tropical Plant Germplasm: Current Research Progress and Applications, (eds) Engelmann F & Takagi H, Japan International Research Center for Agricultural Sciences, Japan & International Plant Genetic Resources Institute, Rome, ISBN: 92–9043-428–7.
26. Fahy GM, MacFarlane DR, Angell CA & Meryman H (1984) Cryobiology 21, 407–426. [PubMed: 6467964]
27. Fahy GM & Rall WF (2007) in Vitrification in Assisted Reproduction, (eds) Tucker MJ & Liebermann J, Informa Healthcare, London, pp. 1–20.
28. Fahy GM, Wowk B & Wu J (2006) Rejuvenation Research 9, 279–291. [PubMed: 16706656]
29. Fahy GM, Wowk B, Wu J, Phan J, Rasch C, Chang A & Zendejas E (2004) Cryobiology 48, 157–178. [PubMed: 15094092]
30. Fowler A & Toner M (2006) Annals of the New York Academy of Sciences 1066, 119–135.
31. Gardner DK & Lane M (2000) in Handbook of In Vitro Fertilization, 2nd Edition, (eds) Trounson AO & Gardner DK, CRC Press, Boca Raton, FL, pp 205–264.

32. Garman E & Mitchell E (1996) Journal of Applied Crystallography 29, 584–587.
33. Hay M & Goodrowe K (1993) Journal of Reproduction and Fertility. Supplement 47, 297–305. [PubMed: 8229940]
34. Hopkins JB, Badeau R, Warkentin M & Thorne RE (2012) Cryobiology 65, 169–178. [PubMed: 22728046]
35. Kalinin Y & Thorne R (2005) Acta Crystallographica Section D: Biological Crystallography 61, 1528–1532. [PubMed: 16239731]
36. Karlsson J, Cravalho E & Toner M (1994) Journal of Applied Physics 75, 4442–4455 (1994).
37. Kartha K, Leung N & Mroginski L (1982) Zeitschrift für Pflanzenphysiologie 107, 133–140.
38. Khosla K, Zhan L, Bhati A, Carley-Clopton A, Hagedorn M & Bischof J (2018) Langmuir 35, 7364–7375. [PubMed: 30299961]
39. Kim H-H, Lee Y-G, Shin D-J, Ko H-C, Gwag J-G, Cho E-G & Engelmann F (2009) CryoLetters 30, 320–334. [PubMed: 19946655]
40. Kloeppel K, Gerlach J & Neuhaus P (1994) Langenbecks Archiv für Chirurgie 379, 329–334. [PubMed: 7845157]
41. Kuleshova L, Macfarlane DR, Trounson AO & Shaw JM (1999) Cryobiology 38, 119–130. [PubMed: 10191035]
42. Kuleshova L, Shaw JM & Trounson AO (2001) Cryobiology 43, 21–31. [PubMed: 11812048]
43. Macfarlane DR (1986) Cryobiology 23, 230–244.
44. MacFarlane DR (1987) Cryobiology 24, 181–195.
45. Manuchehrabadi N, Gao Z, Zhang J, Ring HL, Shao Q, Liu F, McDermott M, Fok A, Rabin Y & Brockbank KG (2017) Science Translational Medicine 9, eaah4586. [PubMed: 28251904]
46. Manuchehrabadi N, Shi M, Roy P, Han Z, Qiu J, Xu F, Lu TJ & Bischof J (2018) Annals of Biomedical Engineering 46, 1857–1869. [PubMed: 29922954]
47. Matsumoto T, Sakai A, Takahashi C & Yamada K (1995) CryoLetters 16, 189–196.
48. McFerrin MB & Snell EH (2002) Journal of Applied Crystallography 35, 538–545.
49. Mehl PM (1993) Cryobiology 30, 509–518. [PubMed: 11987991]
50. Minakov A, Adamovsky S & Schick C (2005) Thermochimica Acta 432, 177–185.
51. Minakov A, Morikawa J, Hashimoto T, Huth H & Schick C (2005) Measurement Science and Technology 17, 199.
52. Minakov AA & Schick C (2007) Review of Scientific Instruments 78, 073902. [PubMed: 17672768]
53. Mullen S & Fahy G (2011) in Principles & Practice of Fertility Preservation, (eds) Donnez J & Kim SS, Cambridge University Press, Cambridge, pp 145–163.
54. Murase N, Fujita T & Gonda K (1983) CryoLetters 4, 19–21.
55. Murase N, Gonda K & Watanabe T (1986) The Journal of Physical Chemistry 90, 5420–5426.
56. Nadarajan J & Pritchard HW (2014) PLoS One 9, e96169. [PubMed: 24788797]
57. Nishizawa S (1992) CryoLetters 13, 379–388.
58. Nishizawa S, Sakai A, Amano Y & Matsuzawa T (1993) Plant Science 91, 67–73.
59. Pathmanathan K & Johari G (1990) Journal of Polymer Science Part B: Polymer Physics 28, 675–689.
60. Peyridieu J, Baudot A, Boutron P, Mazuer J, Odin J, Ray A, Chapelier E, Payen E & Descotes J (1996) Cryobiology 33, 436–446. [PubMed: 8764852]
61. Qin Z & Bischof JC (2012) Chemical Society Reviews 41, 1191–1217. [PubMed: 21947414]
62. Rall WF & Fahy GM (1985) Nature 313, 573. [PubMed: 3969158]
63. Rubinsky B (2003) Heart Failure Reviews 8, 277–284. [PubMed: 12878837]
64. Rubinsky B, Perez PA & Carlson ME (2005) Cryobiology 50, 121–138. [PubMed: 15843002]
65. Sakai A (1995) in Cryopreservation of Plant Germplasm I. Biotechnology in Agriculture and Forestry, vol 32, (ed) Bajaj YPS, Springer, Berlin, Heidelberg, pp. 53–69.
66. Sakai A & Engelmann F (2007) CryoLetters 28, 151–172. [PubMed: 17898904]
67. Sakai A, Kobayashi S & Oiyama I (1990) Plant Cell Reports 9, 30–33. [PubMed: 24226373]

68. Sakai A, Kobayashi S & Oiyama I (1991) Plant Science 74, 243–248.
69. Shaw JM, Kuleshova L, Macfarlane DR & Trounson AO (1997) Cryobiology 35, 219–229. [PubMed: 9367610]
70. Song YC, Khirabadi BS, Lightfoot F, Brockbank KG & Taylor MJ (2000) Nature Biotechnology 18, 296.
71. Songsasen N & Leibo S (1997) Cryobiology 35, 240–254. [PubMed: 9367612]
72. Steponkus P (1992) in Advances in Low Temperature Biology, Vol. 1, (ed.) Steponkus PL, Elsevier Science, pp 1–61.
73. Stott SL & Karlsson JO (2009) Cryobiology 58, 84–95. [PubMed: 19041300]
74. Sutton RL (1991) Journal of the Chemical Society, Faraday Transactions 87, 3747–3751.
75. Sutton RL (1991) Journal of the Chemical Society, Faraday Transactions 87, 101–105.
76. Sutton RL (1992) Cryobiology 29, 585–598. [PubMed: 1424715]
77. Taylor M, Song Y & Brockbank K (2004) in Life in the Frozen State, (eds) Fuller BJ, Lane N & Benson EE, CRC Press, Boca Raton, FL, pp. 604–641.
78. Toner M, Cravalho EG & Karel M (1990) Journal of Applied Physics 67, 1582–1593.
79. Tucker MJ & Liebermann J (2015) (eds) Vitrification in Assisted Reproduction, CRC Press.
80. Uragami A, Sakai A, Nagai M & Takahashi T (1989) Plant Cell Reports 8, 418–421. [PubMed: 24233367]
81. Warkentin M, Stanislavskaia V, Hammes K & Thorne RE (2008) Journal of Applied Crystallography 41, 791–797. [PubMed: 19529833]
82. Webb WR & Karow A (1965) JAMA 191, 1012–1014. [PubMed: 14257727]
83. Weiser C (1970) Science 169, 1269–1278. [PubMed: 17772511]
84. Wowk B, Darwin M, Harris SB, Russell SR & Rasch CM (1999) Cryobiology 39, 215–227. [PubMed: 10600255]
85. Wowk B, Fahy GM, Ahmedyar S, Taylor MJ & Rabin Y (2018) Cryobiology 82, 70–77. [PubMed: 29660316]
86. Yi F, Kim IK, Li S & Lavan DA (2014) Journal of Pharmaceutical Sciences 103, 3442–3447. [PubMed: 25256917]
87. Yi F & LaVan DA (2013) Thermochimica Acta 569, 1–7.
88. Zhuravlev E & Schick C (2010) Thermochimica Acta 505, 1–13.

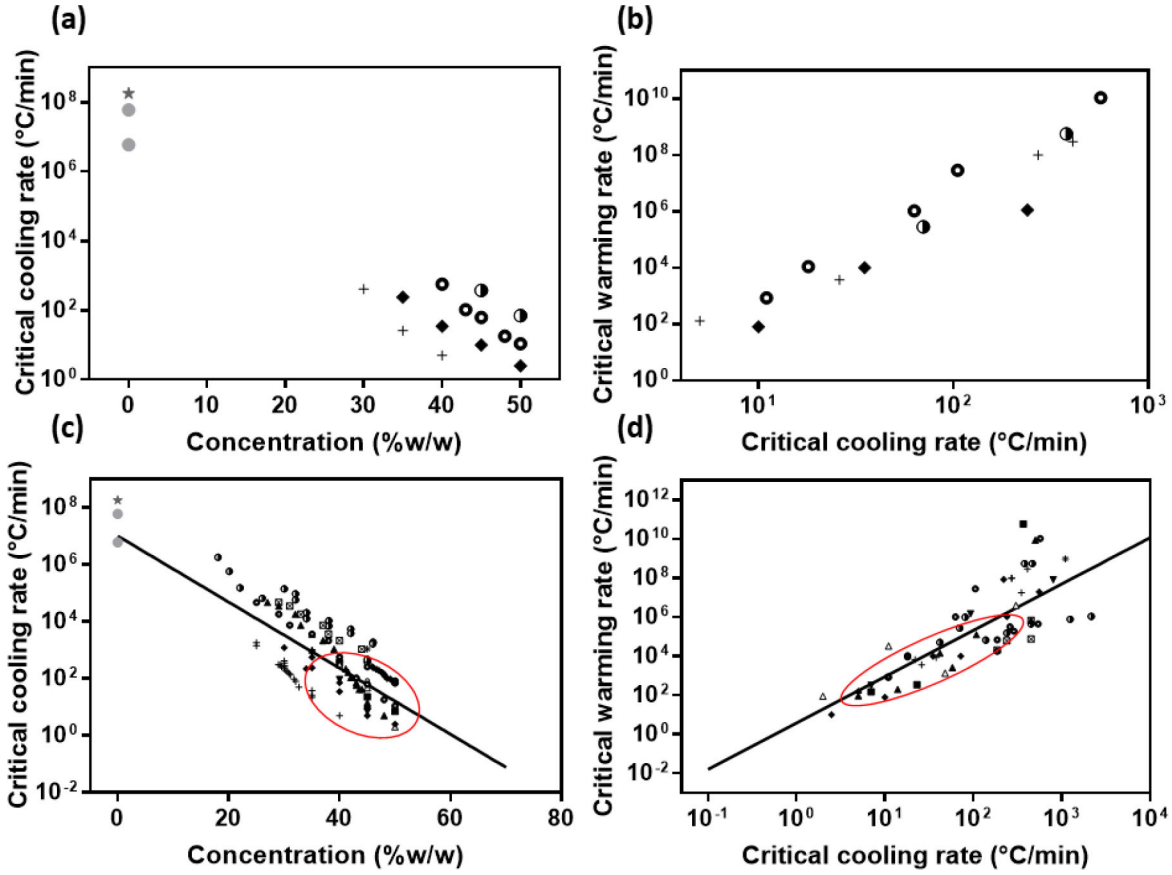

Figure 1.

(a-b) Early study on relationships between CCRs and concentrations, and CWRs and CCRs for solutions of single component CPAs in water (27, 53, 79). **(a)** CCRs for solutions of CPAs in water in relation to their concentrations. **(b)** CWRs as a function of CCRs for solutions of CPAs in water. **(c-d)** The same relationships including more recent data (circle represents the location of the data in Fig. 1a and b). Symbols: ★: Water estimated by Bald (5), 25CF: Water estimated by Bruggeller and Mayer (20), +: 2,3-Butanediol (6, 9, 13, 75), ◆:1,2-Propanediol (6, 9, 74, 84), ○: Ethylene glycol l (6, 8, 11, 34, 84), ▲: Dimethylsulfoxide (DMSO) (6, 11, 34, 75), ◑: Glycerol (6, 34, 81, 84), ▼: 1,3Butanediol (6), ⯅: 1,2,3-Butanetriol (6), △:Diethylformamide (DEF) (6), ■: dimethylformamide (DMF) (6), ♀: 1,4-Butanediol (6), *: 1,3-Propanediol (6), ⊠: PEG 200 (11, 34)

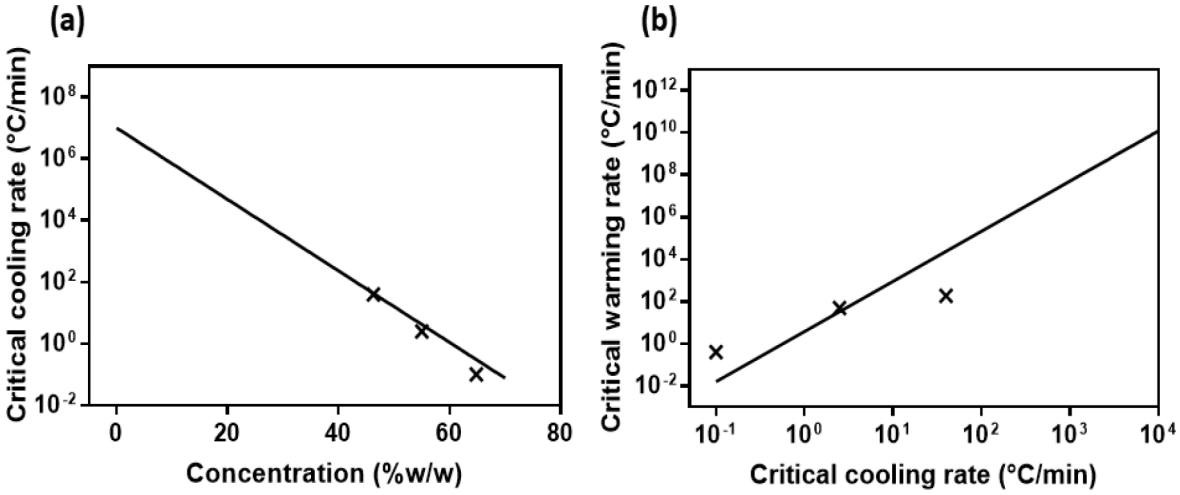

Figure 2.

(a, b) CCR and CWR data points for full concentration CPA cocktails, 6 M DP6, 8.4 M VS55 and 9.345 M M22, and the fitting curves for CPA aqueous solutions.

Table 1.

CCR and CWR measuring methods and maximum rates.

Cooling/warming method	DSC	Plunge cooling/warming	Fast scanning calorimetry	Laser calorimetry
Maximum achievable rates	160 °C/min (2.67 °C/s)	10^5 °C/s	$10^5 \sim 10^6$ °C/s	Cooling: 10^5 °C/s Heating: 10^7 °C/s
Data resources in Fig 1.	(2), (5), (6), (8), (9), (13), (14), (15), (16), (17), (23), (28), (29), (70), (74), (84), (85)	(11), (34), (81)	NA	NA